Injury risk functions for the four primary knee ligaments

Research Article

Corresponding author:
Jiota Nusia [a]
[a] Department of Traffic Safety and Traffic System, Swedish National Road and Transport Research Institute (VTI). **Address**: Malvinas väg 6, 114 28 Stockholm, Sweden.
E-mail: jiota.nusia@vti.se

Co-authors:
Jia Cheng Xu [a]
[a] Department of Traffic Safety and Traffic System, Swedish National Road and Transport Research Institute (VTI). **Address**: Malvinas väg 6, 114 28 Stockholm, Sweden.
E-mail: jia.cheng.xu@vti.se

Reimert Sjöblom [b]
[b] Department of Strength and Crash Analysis (RCCC), Scania CV AB. **Address:** Vagnmakarvägen 1, 151 32 Södertälje, Sweden.
E-mail: reimert.sjoblom@scania.com

Johan Knälmann [b]
[b] Department of Strength and Crash Analysis (RCCC), Scania CV AB. **Address:** Vagnmakarvägen 1, 151 32 Södertälje, Sweden.
E-mail: johan.knalmann@scania.com

Astrid Linder [c]
[c] Department of Traffic Safety and Traffic System, Swedish National Road and Transport Research Institute (VTI). **Address:** Regnbågsgatan 1, 417 55 Gothenburg, Sweden.
E-mail: astrid.linder@vti.se

Svein Kleiven [d]
[d] Department of Biomedical Engineering and Health Systems, KTH Royal Institute of Technology, Stockholm, Sweden. **Address:** Hälsovägen 11, 141 52 Huddinge, Sweden.
E-mail: sveink@kth.se

ABSTRACT

The purpose of this study was to scan the available literature and use the obtained literature data to develop Injury Risk Functions (IRFs) for the Anterior- and Posterior Cruciate Ligament (ACL and PCL, respectively) and the Medial- and Lateral Collateral Ligament (MCL and LCL, respectively) in the knee joint. The IRFs were developed from Post-Mortem Human Subject (PMHS) tensile failure strains of Bone-Ligament-Bone (BLB) or dissected LIGament (LIG) preparations. Insufficient sample size of experimental datapoints required utilization of available literature data by statistically generating failure strains based on mean- and standard deviation from experiments that did not provide specimen-specific results. All virtual and specimen-specific values were then categorised into groups of static and dynamic rates and tested for the best fitting theoretical distribution to formulate the ligament IRF. Nine IRFs were derived (3 for ACL, 2 for PCL, 1 for MCL and 3 for LCL). These IRFs are, to the best of the authors' knowledge, the first attempt at knee ligament injury predicting tools based on PMHS data. For future improvements of the knee ligament IRFs, upcoming experiments should have comparable testing and strain measuring methods, a clear definition of failure and a transparent reporting of each specimen specific result.

KEYWORDS

Injury risk functions, knee ligaments, cruciate ligaments, collateral ligaments.

1 INTRODUCTION

Knee ligament injuries are associated with both low-energy- and high-energy trauma (Schlumberger et al., 2020). Traffic as well as sports related accidents (high- and low-energy trauma, respectively) are two main causes of Anterior- and Posterior Cruciate Ligament injuries (ACL and PCL, respectively) leading to primary reconstructions, both as single injuries as well as multi-ligament injuries (Nicolini et al., 2014; Owesen et al., 2018; Prentice et al., 2018; The Swedish National Knee Ligament Registry, 2019). Although not life-threatening, knee ligament injuries increase the risks of subsequent injuries such as arthritis, meniscus tear and the need for a total knee replacement (Sanders et al., 2017a; Sanders et al., 2017b; Sepúlveda et al., 2017; Wang et al., 2018), reduces the possibility of returning to previous levels of sporting activity (Everhart et al., 2018; Nwachukwu et al., 2019; Sepúlveda et al., 2017) and can have a long-term negative effect on the quality of life (Filbay et al., 2015; Filbay et al. 2018).

The four primary knee ligaments; ACL, PCL and the Medial- and Lateral Collateral Ligaments (MCL and LCL, respectively), are commonly associated with three different injury mechanisms: (1) Mid-section failure is a rupture within the ligament itself; (2) Ligament detachment occurs at the interface between the ligament and the bone, and; (3) Avulsion fractures occur when osseous fragments adjacent to the ligament insertion sites follows as the ligaments detaches (Cho and Kwak, 2020; Lee and Hyman, 2002; Marieswaran et al., 2018; Noyes and Grood, 1976; Paschos et al., 2010; Robinson et al., 2005; White et al., 2013; Winkelstein, 2013). These three different failure modes are a consequence of the interaction between ligament and bone, which have substantially different mechanical properties.

Evaluating the risk for injury can be done using numerical simulations. Finite element Human Body Models (HBMs), such as Total Human Model for Safety (THUMS) and Global Human Body Model Consortium (GHBMC), are expected to increasingly complement testing using physical dummies. HBMs offers the opportunity to evaluate impacts down to tissue level and address occupant diversity to a greater extent than what is practically possible using physical dummies. Local Injury Risk Functions (IRFs) are needed in the evaluation of the knee ligament responses as they predict the risk of injury on a material level, allowing injury mechanisms to be accounted for. Existing human-based IRFs for the lower extremities have primarily been focusing on skeletal fractures (Kuppa et al., 2001; Laituri et al., 2006; Prasad et al., 2010; Rupp et al., 2010; Weaver et al., 2015; Yoganandan et al., 2015), while IRFs for knee ligaments based on human data are missing from the literature. The existing lower extremity IRFs describe the global injury risk of the Knee-Thigh-Hip (KTH) complex (Kuppa et al., 2001; Laituri et al., 2006; Prasad et al., 2010; Rupp et al., 2010), however, they do not address the knee ligament responses as they assume injury risk based only on fracture loads. Knee ligament injuries are dependent on impact location and the IRFs herein might underestimate the risk for KTH injury, by not being sensitive enough to capture knee ligament injuries caused by impact loads below fracture magnitudes (Prasad et al., 2010). Local IRFs of the knee ligaments are needed tools in addressing the ligament impact responses (such as in finite element HBM simulations) and in the development of preventative measures for knee ligament injuries. The objective of this study is to scan the literature for PHMS experimental tensile failure studies of the knee four primary ligaments: ACL, PCL, MCL and LCL; and use the obtained literature data to create local IRFs.

2 METHOD

Cumulative injury risk functions were derived from specimen-specific failure strains in experimental studies conducted on Post-Mortem Human Subject (PMHS) ligaments as previously utilized for hip fracture risk functions by Kleiven (2020). However, most results were provided as averaged failure strains and only a limited number of individual specimen specific strain results were found in literature, entailing insufficient sample information to alone construct IRFs. Therefore, the focus was shifted to utilizing available literature data to construct IRFs by statistically generating failure strains from the provided mean- and Standard Deviation (SD).

2.1 Study search

A literature search was performed for experimental studies conducting uniaxial failure tests on PMHS ligaments. The search was conducted iteratively between February 2019 and April 2021, mainly on Google Scholar. Some of the search words used include “ACL/PCL/MCL/LCL material properties”, “Failure strain”, “Tensile properties”, “Knee joint” in different combinations. Most of the collected studies shown in Table A1 in Appendix A, were found by reviewing the reference list in articles generated by the Google Scholar search.

2.2 Study selection

The inclusion criteria for selecting a study in the development of injury risk functions were: (1) Ligament failure (deformation at maximum load) had to be presented in terms of strain

values, or elongation failures together with initial ligament lengths; (2) conducted on adult PMHS, and; (3) Primary sources of the experiment results, exclusively. Results stating bony fracture or avulsion as failure mode were excluded as they do not represent an injury mechanism on the ligament tissue itself. Table 1 lists all studies meeting these criteria.

Five of these articles provided specimen-specific failure strains (Butler et al., 1992; Kerrigan et al., 2003; Paschos et al., 2010; Smeets et al., 2017, Marieswaran et al. 2021). Wilson (2012) presented failure elongation for each LCL specimen; however, the initial lengths were given as an average. Virtual failure strains were therefore statistically generated from a presented mean failure strain. Van Dommelen (2005) included the results of Kerrigan (2003) in the averaging of LCL failure strains. Hence, to avoid duplication of data, the reported LCL results in Kerrigan (2003) were not applied. Further, van Dommelen (2005) results for MCL were excluded from the current study as the authors' reported that they had used inaccurate initial MCL length in the failure strain calculation. Paschos (2010) strain results at maximum tensile load were extracted from the force-elongation graphs using the online tool WebPlotDigitizer (Rohatgi, 2020).

Study	Mean strain [%]	SD [%]	N	Tensile rate	Specimen	Failure mode
ANTERIOR CRUCIATE LIGAMENT						
Butler (1992) – AMB *	19.1	2.8	5	100 %/s	BLB	Ligament & insertion site
Butler (1992) – ALB *	16.1	3.9	6	100 %/s	BLB	Ligament & insertion site
Butler (1992) – PC *	15.2	5.2	6	100 %/s	BLB	Ligament & insertion site
Chandrashekar (2006) - Male	30.0	6.0	8	100 %/s	BLB	Ligament failure
Chandrashekar (2006) - Female	27.0	8.0	9	100 %/s	BLB	Ligament failure
Nooyes & Grood (1976) - Younger	44.3	8.5	6	100 %/s	BLB	Ligament failure
Van Dommelen (2005) - aACL	18.0	2.8	4	54 ± 9.2 %/s	BLB	Ligament failure
Van Dommelen (2005) - pACL	22.0	3.0	3	63 ± 3.4 %/s	BLB	Ligament failure
Marieswaran (2021) *	45.0	3.0	6	300 %/s	BLB	Insertion site
Marieswaran (2021) *	42.0	2.0	6	30 %/s	BLB	Ligament & insertion site
Paschos (2010) *	42.7	18.5	10	1.5 mm/s	BLB	Ligament & insertion site
Marieswaran (2021) *	44.0	3.0	6	3%/s	BLB	Insertion site
Kennedy (1976)	30.8	2.3	10	2.083 mm/s	LIG	
Kennedy (1976)	35.8	2.8	10	8.33 mm/s	LIG	
POSTERIOR CRUCIATE LIGAMENT						
Butler (1986) – donor 1	14.6	4.6	3	100 %/s	BLB	Ligament failure
Butler (1986) – donor 2	14.0	2.4	2	100 %/s	BLB	Ligament failure
Butler (1986) – donor 3	18.9	2.9	3	100 %/s	BLB	Ligament failure
Race & Amis (1994)– aPCL	18.0	5.3	7	50 %/s	BLB	
Race & Amis (1994) – pPCL	19.5	5.4	10	50 %/s	BLB	
Van Dommelen (2005) - aPCL	18.0	2.3	2	45 ± 5.7 %/s	BLB	Ligament failure
Van Dommelen (2005) - pPCL	14.0	1.4	3	49 ± 5.3 %/s	BLB	Ligament failure
Kennedy (1976)	28.3	1.9	10	2.083 mm/s	LIG	
Kennedy (1976)	24.2	2.1	10	8.33 mm/s	LIG	
MEDIAL COLLATERAL LIGAMENT						
Kerrigan (2003) *	11.5	5.3	3	1205 ± 306 %/s	BLB	Ligament failure
Kerrigan (2003) *	20.3	3.9	3	1.78 ± 0.35 %/s	BLB	Ligament failure
Kennedy (1976)	24.3	1.3	10	8.33 mm/s	LIG	
Kennedy (1976)	23.0	2.4	10	2.083 mm/s	LIG	
Quapp and Weiss (1998)	17.1	1.5	9	1%/s	LIG	
Smeets (2017) *	22.9	2.5	12	2 %/s	LIG	
LATERAL COLLATERAL LIGAMENT						
Butler (1986) – donor 1	10.5	2.5	2	100 %/s	BLB	Ligament failure
Butler (1986) – donor 2	12.7	0.9	2	100 %/s	BLB	Ligament failure
Butler (1986) – donor 3	16.7	3.2	2	100 %/s	BLB	Ligament failure
Kerrigan (2003) *	10.5	4.6	3	1908 %/s	BLB	Ligament failure
LaPrade (2005)	16.0	5.0	8	100 %/s	BLB	Ligament failure
Wilson (2012) *	12.5	2.8	9	20 %/s	BLB	Ligament & insertion site
Smeets (2017) *	41.0	9.9	11	2 %/s	LIG	
Sugita & Amis (2001)	16.1	2.5	9	3.33 mm/s	BLB	
Van Dommelen (2003)	15.0	2.9	4	≤0.001 %/s	BLB	Ligament failure
Van Dommelen (2003)	20.0	5.5	6	0.04 ±0.009 %/s	BLB	Ligament failure

TABLE 1. *Mean failure strains ± SD as reported by studies used to construct the injury risk functions. The uniaxial tensile tests were conducted on either Bone-Ligament-Bone (BLB) specimens or dissected Ligaments*

(LIG). The studies are grouped according to dynamic (red) or static (green) tensile rate. "N" represents the number of specimens used in the averaging while "Failure mode" specifies the injury mechanisms of the BLB specimens; (1) Mid-substance ligament failure, or (2) Failure at ligament attachment site. Empty boxes indicate that the information was not presented.
**Specimen-specific results provided.*

2.3 Categorisation of dataset

The injury risk functions were generated based on whether the experiments were conducted on Bone-Ligament-Bone (BLB) specimens or on dissected LIGament samples (LIG), as the two specimen types differ in which of the failure mechanisms they employ. To act for the viscoelastic characteristics of the ligaments (Winkelstein, 2013), the studies were further categorised into two subgroups, depending on whether they conducted the tensile test using strain rates below (labelled "static") or equal and above (labelled "dynamic") 10 %/s. IRFs were generated for sample sizes of at least 10 failure strains, Table 2 gives an overview of their characteristics and Figure 1 illustrates the construction procedure of the IRFs.

LIGAMENT	RATE (DYN/STATIC)	SPECIMEN (BLB/LIG)	FAILURE STRAIN VALUES (Virtual/ Specimen-specific/Mix)	SAMPLE SIZE
ACL	DYNAMIC	BLB	MIX	59
ACL	STATIC	BLB	SPECIMEN-SPECIFIC	16
ACL	STATIC	LIG	VIRTUAL	20
PCL	DYNAMIC	BLB	VIRTUAL	30
PCL	STATIC	LIG	VIRTUAL	20
MCL	STATIC	LIG	MIX	41
LCL	DYNAMIC	BLB	MIX	26
LCL	STATIC	BLB	VIRTUAL	19
LCL	STATIC	LIG	SPECIMEN-SPECIFIC	11

TABLE 2. *Nine injury risk functions (IRFs) were generated representing either Bone-Ligament-Bone (BLB) specimens or dissected Ligament samples (LIG), studied in a tensile rate either below ("static") or equal and above ("dynamic") 10%/s. The IRFs were composed of either virtually generated values, specimen-specific values, or a mix of the two.*

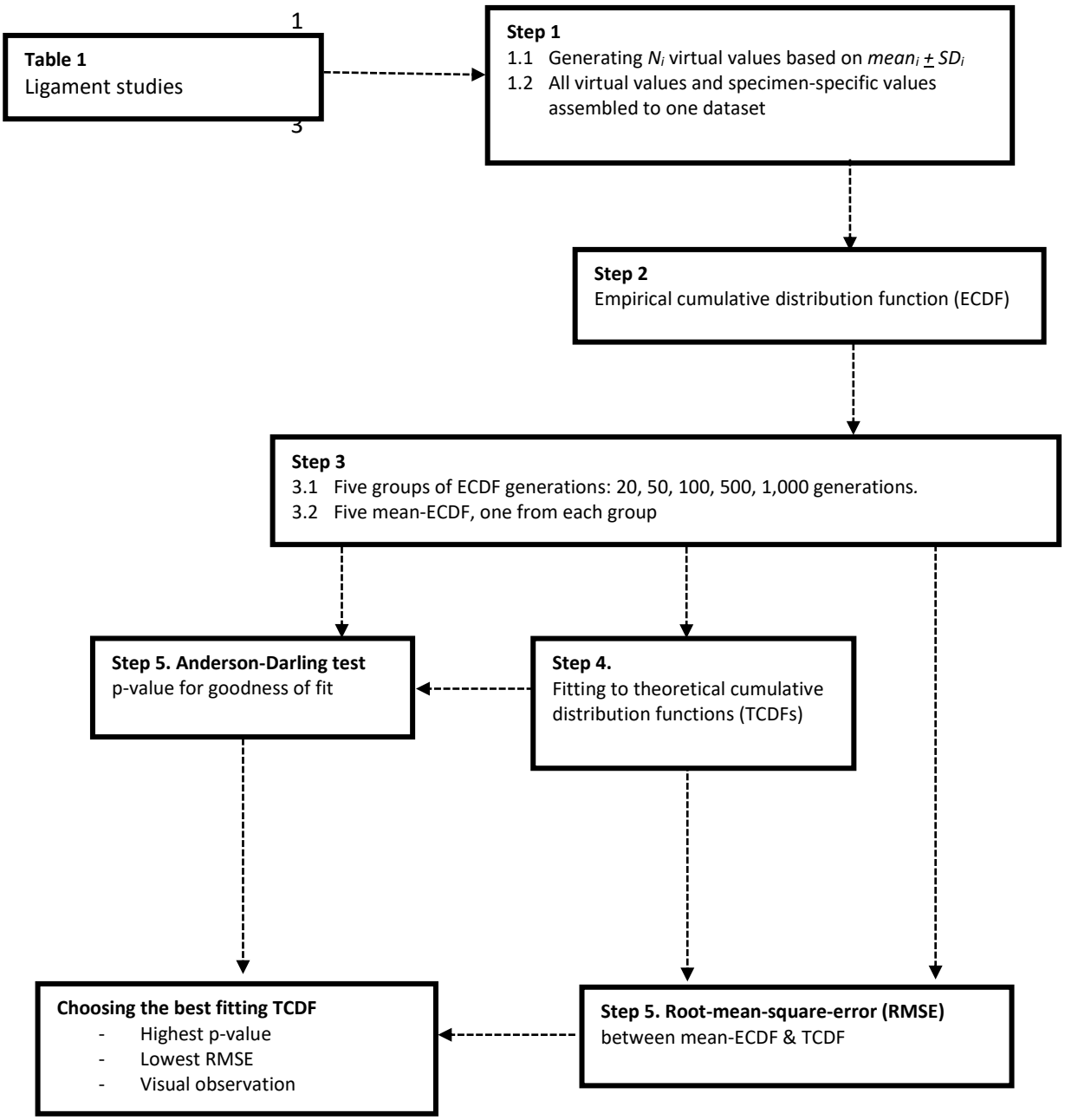

Figure 1. *The process of constructing the injury risk functions. Experimental values were statistically generated based on studies of mean ± SD that did not provide specimen specific failure strain results (Step 1). The virtual values of all studies were thereafter assembled with the provided specimen specific results to collectively represent the dataset for one risk function (Step 2). Five groups composed of 20-1,000 generations of ECDFs were generated with five corresponding mean-ECDF's calculated representing each group (Step 3). Each mean-ECDF was tested against various theoretical distributions, and their corresponding TCDF were generated (Step 4). The best fitting TCDF was chosen based on the theoretical distribution's goodness of fit using the Anderson-Darling test, on the root-mean-square error (RMSE) between the mean-ECDF and on the TCDF and visual observations (Step 5).*

2.4 Generating virtual values

The failure strains used for the generation of virtual values (Table 1) were assumed to be normally distributed because that the results were presented as mean- and SD only. If not stated otherwise, all strains were furthermore assumed to be engineering strains and were converted to Green-Lagrange strain (ε), Eq. (1) and the Box-Müller basic transform (Box and Muller, 1958) was adopted for the generation of normally distributed virtual values, Eq. (2):

$$\varepsilon = \frac{1}{2}(\lambda^2 - 1) \qquad (1)$$

$$Z = \sqrt{-2\ln(U_1)} * \cos(2\pi U_2) \qquad (2)$$

$$X_{virtual} = Z * \varepsilon_{SDi} + \varepsilon_{MEANi} \qquad (3)$$

where λ is the stretch ratio. U_1 and U_2 are two series of independent random variables, uniformly distributed in the interval [0,1] and corresponding to each study$_i$'s sample size *N*, Table 1. *Z* is a set with the resulting independent random variables having a normal distribution and a mean value at zero $\pm$ one unit SD, which was then shifted to match each study's mean failure strains and SD, Eq. (3). Conclusively, $X_{virtual}$ is a collection of *N* statistically estimated failure strains, corresponding to the study's ε_{MEANi} and ε_{SDi} . All $X_{virtual}$ from each study (including the specimen-specific results if provided) were assembled in one dataset to derive one risk function.

2.5 Constructing injury risk functions

As the values in $X_{virtual}$ were randomly generated failure strains within the range of every ε_{MEANi} and ε_{SDi} , the robustness of the method was evaluated by generating groups of 20,

50, 100, 500 and 1,000 Empirical Cumulative Distribution Functions (ECDFs) for each ligament. The analysis was based on calculated mean-ECDFs representing each group of ECDF generations with respect to the injury risk. Theoretical (parametric) distributions commonly used within survival analysis (George et al., 2014) were fitted against the mean-ECDF of all five groups by using the MATLAB function "fitdist", and the goodness of fit was evaluated with the Anderson-Darling test[36] (AD-test). The best fitting probability distribution function was chosen to derive the cumulative distribution function, to define the risk of failure based on strain. Theoretical Cumulative Distribution Functions (TCDFs) were chosen to formulate each ligaments injury risk function. The evaluation was based on: (1) the largest p-values from the AD-test; (2) the lowest Root-Mean-Square Error (RMSE) between the mean-ECDF and each distribution's corresponding TCDF, and; (3) visual observation of the plotted curves (Figure 1). The visual observation aimed to control for good fit primarily for the lower risk levels, as they are of most relevance in injury evaluation. The parameters in the cumulative distribution function of the chosen theoretical distribution were defined based on the smallest confidence interval between the five generation groups.

Student's T-Test was used to evaluate the influence of strain rate on the failure threshold if the BLB IRF derived for static and dynamic rates, namely ACL-dynamic-BLB vs. ACL-static-BLB and LCL-dynamic-BLB vs. LCL-static-BLB. The null hypothesis was rejected for p-values ≤ 0.05 – stating a statistical strain rate dependency of the datasets.

3 RESULTS

Fifteen publications met the inclusion criteria for the generation of nine IRFs. Of the tested distributions, the Log-Logistic and Weibull showed the best fit to the empirical dataset. Table 3 summarises the resulting p-values and RMSE for the chosen generation group of the best fitting distribution, most ranging above 0.9 and between 2.3 - 4.7 %, respectively.

Injury risk function	Distribution	Scale parameter, α	Shape parameter, β	p-value	RMSE [%]	Generation group
ACL DYNAMIC BLB	Log-Logistic	29.93 (26.14 – 34.26)	3.46 (2.79– 4.30)	0.854	6.96	100
ACL STATIC BLB	Log-Logistic	50.28 (40.64 – 62.2)	4.14 (2.71 – 6.32)	0.907	7.74	-
ACL STATIC LIG	Log-Logistic	38.64 (36.78 - 40.59)	15.85 (11.11 - 22.61)	0.992	4.29	100
PCL DYNAMIC BLB	Log-Logistic	18.62 (16.88 - 20.54)	6.39 (4.76 - 8.59)	0.999	2.33	500
PCL STATIC LIG	Weibull	31.15 (29.83 - 32.53)	10.68 (7.58 - 15.05)	0.995	4.68	500
MCL STATIC LIG	Weibull	26.10 (24.91 - 7.34)	7.19 (5.60 - 9.23)	0.955	3.68	100
LCL DYNAMIC BLB	Log-Logistic	13.90 (12.40 - 15.59)	5.65 (4.11 - 7.78)	0.999	2.59	500
LCL STATIC BLB	Log-Logistic	18.12 (16.41 - 20.01)	7.90 (5.43 - 11.48)	1	2.86	100
LCL STATIC LIG	Log-Logistic	40.21 (35.47 - 45.58)	8.58 (5.11 - 14.42)	0.971	10.2	-

TABLE 3. *Log-logistic and Weibull shape and scale parameters for the nine IRFs representing the cruciate (ACL and PCL) and collateral (MCL and LCL) ligaments. The 95 % confidence intervals are presented within brackets. Resulting p-value for the goodness of fit in the Anderson-Darling test and the Root-Mean-Square-Error (RMSE) is given for the best fitting distribution of the chosen generation group.*

One MCL injury risk function was generated for the static rate only due to the insufficiently large dynamic dataset meeting the inclusion criteria. The Weibull distribution was selected to represent the MCL-static-LIG IRF, having both the statistical results (p-value=0.96, RMSE=3.7 %) and the visual observation confirming the fit between the two clusters of the failure strains at the lower end of the ECDF. All ACL and PCL IRFs had slightly higher p-values and/or lower RMSE for the Gamma or Log-Normal distributions, compared to the chosen distribution (Table B1, Appendix B). However, the visual observations found the differences in the fit to be prominent and mainly located in the upper end of all the IRFs (above 60% of risk), whereas the lower end fitted equally well or better for the Log-logistic or Weibull distributions. As the lower end of an IRF is more applicable for injury prevention, the selected two distributions were chosen in favour for the simplicity of their IRFs'.

The IRF of Weibull and Log-logistic distribution are expressed in Eq. (4) and Eq, (5) and visualised in Figure 2. Table 3 presents the resulting parameters for the chosen group of ECDF generations.

Weibull CDF: $$F(\varepsilon) = 1 - e^{-(\varepsilon/\alpha)^{\beta}} \quad (4)$$

Log-Logistic CDF: $$F(\varepsilon) = \varepsilon^{\beta} \big/ (\varepsilon^{\beta} + \alpha^{\beta}) \quad (5)$$

where ε is the Green-Lagrange strain, α the scale parameter and β the shape parameter.

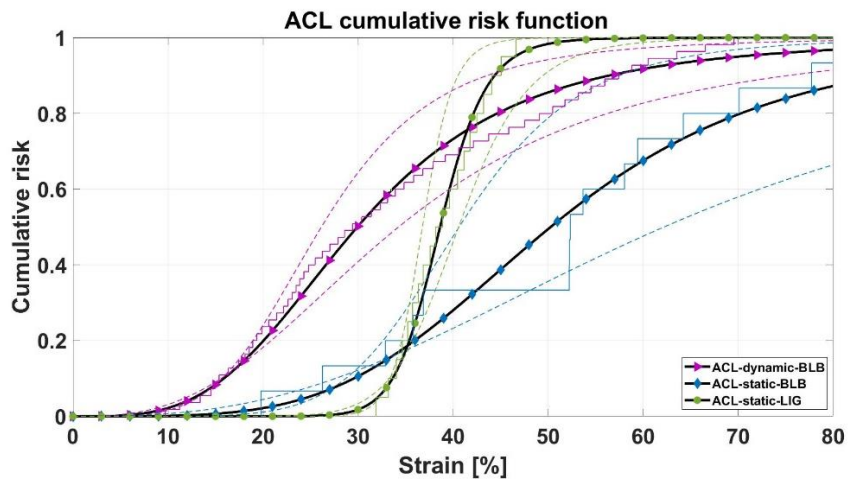

Figure 2.A *Anterior Cruciate Ligament injury risk functions.*

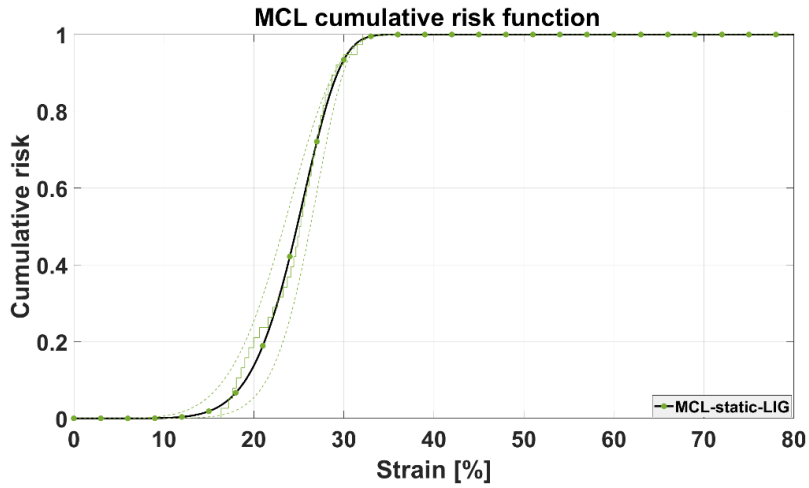

Figure 2.B *Medial Collateral Ligament injury risk function.*

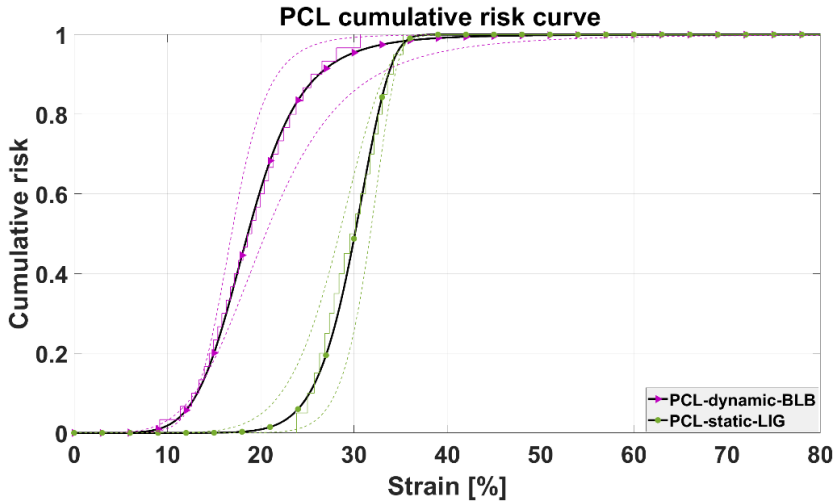

Figure 2.C *Posterior Cruciate Ligament injury risk functions.*

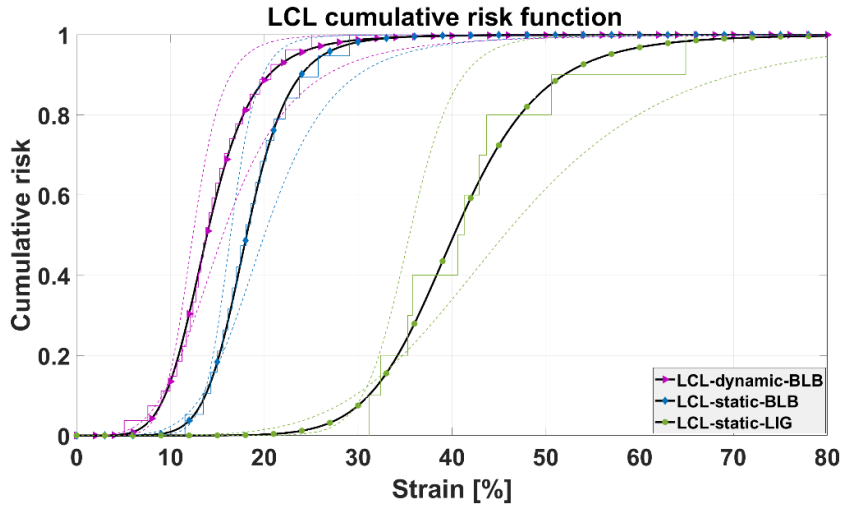

Figure 2.D *Lateral Collateral Ligament injury risk functions.*

Figure 2. *Nine cumulative injury risk functions (IRFs) with 95 % confidence intervals (dotted lines) generated from corresponding mean-ECDF. Derived from failure strains of PMHS ACL, PCL, MCL and LCL specimens, the IRFs are representing either bone-ligament-bone (BLB) or dissected ligament preparations (LIG), tested in either dynamic or static rate. One experimental datapoint in the ACL-static-BLB mean-ECDF reached 112 % failure strain and is therefore not visualised in Figure 2.A.*

Student's T-test analysis confirmed a statistical strain rate dependency between ACL-dynamic-BLB and ACL-static-BLB risk functions ($p<0.001$) and between LCL-dynamic-BLB and LCL-static-BLB ($p=0.004$). Results from Wilson (2012), who conducted LCL tensile tests at approximately 20 %/s strain rate, were included in the dynamic rate group as the failure strains showed statistical strain rate dependency to the LCL-static-BLB dataset ($p=0.001$) and no statistical rate dependency to the dynamic dataset ($p=0.173$). The rate dependency was also confirmed ($p=0.024$) between the dynamic and static BLB datasets with Wilson (2012) excluded, assuring that any rate dependency between them is not driven by Wilson (2012).

4 DISCUSSION

This study provides currently lacking risk functions for the four primary knee ligaments. Nine injury risk functions were derived based on mean failure tensile strains conducted on PMHS ACL, PCL, MCL and LCL specimens. With the exception of MCL, all ligaments have at least one IRF representing either BLB or LIG specimens tested in either the dynamic or static rate. Dynamic IRF was not derived for MCL due to an insufficient number of studies meeting the inclusion criteria.

4.1 The cruciate ligaments

Most studies conducting tensile failure test on ACL and PCL, Table A1 in Appendix A, used BLB specimen preparations. Opposed to the PCL studies, several ACL studies (Chandrashekar et al., 2006; Jones et al., 1995; Marieswaran et al., 2018 & 2021; Noyes and Grood, 1976; Paschos et al., 2010; Trent et al., 1976; Woo et al., 1991) conducted the testing on the whole

ligament, denoted Femur – ACL – Tibia – Complex (FATC); i.e., not separating the ligament into anterior and posterior bundles. The FATC results used in the current study applied the load along the ACL axis (Chandrashekar et al., 2006; Noyes and Grood, 1976; Marieswaran et al. 2021; Paschos et al., 2010). However, as the two bundles of the ACL vary in orientation inside the knee joint, loading the ligament in the longitudinal direction along both bundles was challenging (Woo et al., 1991). Paschos (2010) defined three different failure patterns of the ACL, based on the failure sequences of the bundles. Observing double peaks in the force-elongation graphs, Paschos (2010) demonstrated the role of ACL as a multifiber ligament, by showing that the two bundles did not rupture simultaneously during loading. Woo (1991) further observed that the structural properties and the failure modes (bone avulsion, ligament attachment site and mid-substance failure) in the FATC were affected depending on the tensile load alignment along the ligament. The two knee orientations tested by Woo (1991) showed both a difference in load uptake by the whole ligament, as well as uneven load distribution within the ACL, indicating that ACL failure is sensitive to knee orientation during uniaxial tensile tests.

Observing that all the FATC studies used in the current study present the largest failure strains compared to the other ACL studies (Table 1), there is reason to suspect an interaction between the two bundles, compensating each other by picking up the load during failure. To control for this issue, concerning both cruciate ligaments, future experiments are suggested to measure the distribution of the tensile load between the posterior and anterior bundles.

4.2 The collateral ligaments

The LCL IRFs showed a distinct separation between the two IRFs representing BLB specimens and the IRF for dissected ligaments. The strain at mean risk of failure is approximately double the magnitude of the LCL-static-LIG compared to LCL-static-BLB. Similar proportions were observed by Robinson (2005), comparing MCL failure loads between BLB complexes and dissected ligaments. The two static ACL IRFs did, however, not show this correlation as the ACL-static-LIG demonstrated higher injury risks at lower failure strains compared to the ACL-static-BLB. Although no conclusions can be drawn from the above observations, it is possible that failure at attachment sites might occur prior to mid-substance failures, at least for the collateral ligaments.

The MCL IRF showed a statistically good fit with the MCL dataset, however, observing the mean-ECDF in Figure 2B, the dataset appears to not align with the expected strain behaviour of the tissue. The “bump” on the lower end of the mean-ECDF caused a modest fitting of the MCL IRF and increased the RMSE value, which is presumably induced by the failure strains reported by Quapp and Weiss (1998). Interpretating their analysis of the behaviour of the ligaments at time of failure, it is possible that failure was defined at the time a ligament visibly entered the yield point, which would explain the lower failure strains in their study compared to the other studies.

4.3 Failure mechanisms and tensile rate

Literature data has assumed homogeneity of the ligaments, and therefore also the current study in the construction of the IRFs. The defined tensile rate in most articles refers to the applied actuator displacement rate and not to the resulting ligament strain rate. That is, the displacement rate of the attachment grips has been assumed in the experiments to correspond to the ligaments actual strain rate. This assumption might be applicable for the dissected ligaments; however, it is not obvious for the BLB components. As these specimens are a complex mix of bone and ligament, an additional variety of failure modes comes with including the ligament attachments in the test setup. The flaw of such simplification can be exemplified with ligament failures occurring at one attachment site and rarely in both of a BLB complex, suggesting that the strains vary across a ligament during uniaxial loading (Cho and Kwak, 2020; Paschos et al., 2010; Robinson et al., 2005; Wijdicks et al., 2010).

Nevertheless, studies experimenting on dissected ligaments exclude the insertion site failure mode by taking the ligament out of its environmental context. However, on the other hand, they gain in precision by distinctively addressing only the mid-ligament failures. BLB complexes address both failure modes although the challenge of linking the failure strain to a specific injury mechanism increases. Some studies suggest that failure at the attachment sites occur prior to mid-ligament failure (Noyes and Grood, 1976; Robinson et al., 2005). Other studies indicate rate dependence of the failure modes (Lee and Hyman, 2002; van Dommelen et al., 2005) which supports the requirement of local failure strains to address injury mechanisms in future studies.

4.4 Recommendations for use and future improvements

The IRFs developed in this study are, to the best of the authors knowledge, the first attempt at knee ligament injury predicting tools based on PMHSs.

Analyzing the injury risk of simulated HBMs knee ligament responses, the boundary conditions will most often involve the ligament attached to the bones, making BLB IRFs the most relevant for traffic- and sport related accidents reconstructions. However, apart from providing IRFs, the current study highlights available content in the literature and the IRFs of the LIG specimens are believed to be valuable while assessing risk for failure in investigations other than virtual simulations. In addition, the two specimen types address a variety of failure modes and so the generated IRFs of BLB and LIG should not be compared between the two specimen preparations. The dynamic IRFs are of particular use in injury prediction of knee ligaments, as most (low- and high-energy) accidents are not likely to cause ligament loading in static rates. Although both collateral ligaments have a similar restraining function of the knee joint, enough literature has not been found supporting that the structural properties in the MCL and LCL ligaments are similar in the dynamic rate. Hence, a dynamic BLB IRF representing MCL is needed for injury prediction of higher loading rates and larger set of dynamic MCL datapoints are needed before this IRF can be provided.

As indicated in the beginning of subchapter 4.3, the IRFs should be compared to the crosshead strain of the whole ligament as the literature in the current study measured neither local strain rate nor local failure strains for each tested specimen, which are required

to advance the IRFs. Local failure strain datasets would facilitate more refined loading rate arrangements, as well as addressing covariates that most likely affects the material properties of ligaments, such as age and gender (Chandrashekar et al., 2006; Cho and Kwak, 2020; Noyes and Grood, 1976; Schmidt et al., 2019; Winkelstein, 2013; Woo et al., 1991), which was not possible in the current study due to these literature limitations. To conduct these analyses, there is a need for consistent specification of each specimens' age and sex.

The current study method was formulated to utilize available literature data for generating knee ligament IRFs, because of insufficiently detailed results provided by the articles. IRFs are ideally developed based on PMHS specimen specific data from studies with comparable testing and measuring methods, and with a clear definition of ligament failure. Most experiments used to generate these IRFs deviated in all these factors, and thereby adding complexity in finding uniform arrangements of the dataset. The issue of incomplete data information is probably not unique for knee ligaments, but most likely also present for other tissue and body parts as well. The method of generating virtual failure strains from a mean- and SD could therefore have potential as a valuable alternative method, and should be prioritized to be validated. The provided IRFs, furthermore, need to be evaluated for their ability to predict injury, e.g., by reconstructing known injurious and non-injurious scenarios using HBMs.

5 CONCLUSION

This study provides a first attempt at injury risk functions for the four primary knee ligaments. Developed on tensile failure strains of PMHS specimens; ACL, PCL and LCL were each represented by at least one IRF of dynamic and static tensile rate, respectively. Only limited literature of MCL in dynamic rates met the inclusion criteria, hence only one IRF for static rates was generated. Most of the literature data were provided as averaged failure strains, entailing insufficient sample information to alone construct IRFs. By statistically approximating failure strains from each averaged strain results, the current study utilized available literature data in the construction of the knee ligament IRFs. For future improvements of the knee ligament IRFs, several important factors are required from the literature and upcoming experiments; comparable testing and strain measuring methods, a clear definition of failure and a transparent reporting of each specimen specific result.

STUDY HIGLIGHTS

- First human-based injury risk functions (IRFs) for the four primary knee ligaments.
- Statistical failure strains utilized the available, but limited, literature data.
- Nine IRFs were developed, categorised by tensile strain rate and specimen preparation.
- Future improvements require unified experiment methods and transparent reporting.

ACKNOWLEDGEMENTS

The development of the study and the writing of the manuscript for scientific publication was funded by the VIRTUAL (Open Access Virtual Testing Protocols for Enhances Road User Safety) project, which in turn received funding from the European Union Horizon 2020 Research and Innovation Programme under Grant Agreement No768960. The funder had no role in the study design, data collection, analysis, writing of the report or in the decision of submitting for publication. SK has partly been financed by Vinnova (Swedish Governmental Agency for Innovation Systems, D.nr. 2017-03070 and 2019-03386).

The authors would like to thank Elisabeth Agar for the support with the language review.

REFERENCE LIST

Anderson TW, Darling DA. Asymptotic theory of certain" goodness of fit" criteria based on stochastic processes. *The annals of mathematical statistics.* 1952;23(2):193-212.

Box GEP, Muller MEA. Note on the Generation of Random Normal Deviates. *The Annals of Mathematical Statistics.* 1958;29(2):610-611. http://dx.doi.org/10.1214/aoms/1177706645

Butler DL, Kay MD, Stouffer DC. Comparison of material properties in fascicle-bone units from human patellar tendon and knee ligaments. *J Biomech*. 1986;19(6):425-432. doi:10.1016/0021-9290(86)90019-9

Butler DL, Guan Y, Kay MD, et al. Location-dependent variations in the material properties of the anterior cruciate ligament. *J Biomech*. 1992;25(5):511-518. doi:10.1016/0021-9290(92)90091-e

Chandrashekar N, Mansouri H, Slauterbeck J, et al. Sex-based differences in the tensile properties of the human anterior cruciate ligament. *J Biomech*. 2006;39(16):2943-2950. doi:10.1016/j.jbiomech.2005.10.031

Cho H-J, Kwak D-S. Mechanical Properties and Characteristics of the Anterolateral and Collateral Ligaments of the Knee. *Appl Sci.* 2020; 10(18):6266. https://doi.org/10.3390/app10186266

Everhart JS, Du A, Chalasani R, et al. Return to Work or Sport After Multiligament Knee Injury: A Systematic Review of 21 Studies and 524 Patients. *Arthroscopy*. 2018;34(5):1708-1716. doi:10.1016/j.arthro.2017.12.025

Filbay SR, Ackerman IN, Dhupelia S, et al. Quality of Life in Symptomatic Individuals After Anterior Cruciate Ligament Reconstruction, With and Without Radiographic Knee

Osteoarthritis. *J Orthop Sports Phys Ther*. 2018;48(5):398-408. doi:10.2519/jospt.2018.7830

Filbay SR, Culvenor AG, Ackerman IN et al. Quality of life in anterior cruciate ligament-deficient individuals: a systematic review and meta-analysis. *Br J Sports Med*. 2015;49(16):1033-1041. doi:10.1136/bjsports-2015-094864

George B, Seals S, Aban I. Survival analysis and regression models. *J Nucl Cardiol*. 2014;21(4):686-694. doi:10.1007/s12350-014-9908-2

Jones RS, Nawana NS, Pearcy MJ, et al. Mechanical properties of the human anterior cruciate ligament. *Clin Biomech (Bristol, Avon)*. 1995;10(7):339-344. doi:10.1016/0268-0033(95)98193-x

Kennedy JC, Hawkins RJ, Willis RB, et al. Tension studies of human knee ligaments. Yield point, ultimate failure, and disruption of the cruciate and tibial collateral ligaments. *J Bone Joint Surg Am*. 1976;58(3):350-355.

Kerrigan JR, Ivarsson B, Bose D, et al. Rate-sensitive constitutive and failure properties of human collateral knee ligaments. *In Proc. IRCOBI Conf* 2003;177-190

Kleiven, S. Hip fracture risk functions for elderly men and women in sideways falls. *J Biomech*.2020;105. doi: 10.1016/j.jbiomech.2020.109771

Kuppa, S., Wang, J., Haffner, M., et al. Lower extremity injuries and associated injury criteria. *SAE Technical Paper* (2001). No. 2001-06-0160.

Laituri TR, Henry S, Sullivan K, Prasad P. Derivation and theoretical assessment of a set of biomechanics-based, AIS2+ risk equations for the knee-thigh-hip complex. *Stapp Car Crash J*. 2006;50:97-130.

LaPrade RF, Bollom TS, Wentorf FA, et al. Mechanical properties of the posterolateral structures of the knee. *Am J Sports Med*. 2005;33(9):1386-1391. doi:10.1177/0363546504274143

Lee M, Hyman W. Modeling of failure mode in knee ligaments depending on the strain rate. *BMC Musculoskelet Disord*. 2002;3:3. doi:10.1186/1471-2474-3-3

Marieswaran M, Mansoori N, Digge VK, et al. Effect of preservation methods on tensile properties of human femur-ACL-tibial complex (FATC) - a cadaveric study on male subjects. *Acta Bioeng Biomech*. 2018;20(4):31-42.

Marieswaran M, Sikidar A, Rana Aet al. A cadaveric study on the rate of strain-dependent behaviour of human anterior cruciate ligament *Acta Bioeng Biomech*. 2021;23(1):45-57. doi: 10.37190/ABB-01672-2020-05

Nicolini AP, de Carvalho RT, Matsuda MM, et al. Common injuries in athletes' knee: experience of a specialized center. *Acta Ortop Bras*. 2014;22(3):127-131. doi:10.1590/1413-78522014220300475.

Noyes FR, Grood ES. The strength of the anterior cruciate ligament in humans and Rhesus monkeys. *J Bone Joint Surg Am*. 1976;58(8):1074-1082.

Nwachukwu BU, Adjei J, Rauck RC, et al. How Much Do Psychological Factors Affect Lack of Return to Play After Anterior Cruciate Ligament Reconstruction? A Systematic Review. *Orthop J Sports Med*. 2019;7(5):2325967119845313. Published 2019 May 22. doi:10.1177/2325967119845313

Owesen C, Røtterud JH, Engebretsen L, et al. Effect of Activity at Time of Injury and Concomitant Ligament Injuries on Patient-Reported Outcome After Posterior Cruciate Ligament Reconstruction. *Orthop J Sports Med*. 2018;6(12):2325967118817297. Published 2018 Dec 28. doi:10.1177/2325967118817297

Paschos NK, Gartzonikas D, Barkoula NM, et al. Cadaveric study of anterior cruciate ligament failure patterns under uniaxial tension along the ligament. *Arthroscopy*. 2010;26(7):957-967. doi:10.1016/j.arthro.2009.12.013.

Prasad P, Mertz HJ, Dalmotas DJ et al. Evaluation of the field relevance of several injury risk functions. *Stapp Car Crash J*. 2010;54:49-72.

Prentice HA, Lind M, Mouton C, et al. Patient demographic and surgical characteristics in anterior cruciate ligament reconstruction: a description of registries from six countries. *Br J Sports Med*. 2018;52(11):716-722. doi:10.1136/bjsports-2017-098674

Quapp KM, Weiss JA. Material characterization of human medial collateral ligament. *J Biomech Eng*. 1998;120(6):757-763. doi:10.1115/1.2834890

Race A, Amis AA. The mechanical properties of the two bundles of the human posterior cruciate ligament. *J Biomech*. 1994;27(1):13-24. doi:10.1016/0021-9290(94)90028-0

Robinson JR, Bull AM, Amis AA. Structural properties of the medial collateral ligament complex of the human knee. *J Biomech*. 2005;38(5):1067-1074. doi:10.1016/j.jbiomech.2004.05.034

Rohatgi, A. (November 2020). *WebPlotDigitizer: Version 4.4*. https://automeris.io/WebPlotDigitizer

Rupp JD, Flannagan CA, Kuppa SM. Injury risk curves for the skeletal knee-thigh-hip complex for knee-impact loading. *Accid Anal Prev*. 2010;42(1):153-158. doi: 10.1016/j.aap.2009.07.014

Sanders TL, Pareek A, Barrett IJ, et al. Incidence and long-term follow-up of isolated posterior cruciate ligament tears. *Knee Surg Sports Traumatol Arthrosc*. 2017a;25(10):3017-3023. doi: 10.1007/s00167-016-4052-y

Sanders TL, Pareek A, Kremers HM, et al. Long-term follow-up of isolated ACL tears treated without ligament reconstruction. *Knee Surg Sports Traumatol Arthrosc*. 2017b;25(2):493-500. doi:10.1007/s00167-016-4172-4.

Schlumberger M, Schuster P, Eichinger M, et al. Posterior cruciate ligament lesions are mainly present as combined lesions even in sports injuries. *Knee Surg Sports Traumatol Arthrosc*. 2020;28(7):2091-2098. doi:10.1007/s00167-020-05919-4

Schmidt EC, Chin M, Aoyama JT, et al. Mechanical and Microstructural Properties of Native Pediatric Posterior Cruciate and Collateral Ligaments. *Orthop J Sports Med*. 2019;7(2):2325967118824400. doi:10.1177/2325967118824400

Smeets K, Slane J, Scheys L, et al. Mechanical Analysis of Extra-Articular Knee Ligaments. Part One: Native knee ligaments. *Knee*. 2017;24(5):949-956. doi:10.1016/j.knee.2017.07.013

Sepúlveda F, Sánchez L, Amy E, Micheo W. Anterior Cruciate Ligament Injury: Return to Play, Function and Long-Term Considerations. *Curr Sports Med Rep*. 2017;16(3):172-178. doi:10.1249/JSR.0000000000000356

Sugita T, Amis AA. Anatomic and biomechanical study of the lateral collateral and popliteofibular ligaments. *Am J Sports Med*. 2001;29(4):466-472. doi:10.1177/03635465010290041501

The Swedish National Knee Ligament Registry. *Annual Report 2019*. https://www.aclregister.nu/media/uploads/Annual%20reports/a%CC%8Arsrapport_korsband_2019_eng_040720.pdf (accessed 17 July 2021)

Trent PS, Walker PS, Wolf B. Ligament length patterns, strength, and rotational axes of the knee joint. *Clin Orthop Relat Res*. 1976;(117):263-270.

van Dommelen J, Ivarsson B, Minary Jolandan M, et al. Characterization of the Rate-Dependent Mechanical Properties and Failure of Human Knee Ligaments. *SAE Technical Paper* (2005). No. 2005-01-0293. https://doi.org/10.4271/2005-01-0293

Wang SH, Chien WC, Chung CH, et al. Long-term results of posterior cruciate ligament tear with or without reconstruction: A nationwide, population-based cohort study. *PLoS One*. 2018;13(10):e0205118. Published 2018 Oct 3. doi:10.1371/journal.pone.0205118

Weaver AA, Talton JW, Barnard RT, et al. Estimated injury risk for specific injuries and body regions in frontal motor vehicle crashes. *Traffic Inj Prev*. 2015;16 Suppl 1:S108-S116. doi:10.1080/15389588.2015.1012664

White EA, Patel DB, Matcuk GR, et al. Cruciate ligament avulsion fractures: anatomy, biomechanics, injury patterns, and approach to management. *Emerg Radiol*. 2013;20(5):429-440. doi:10.1007/s10140-013-1121-0

Wijdicks CA, Ewart DT, Nuckley DJ, et al. Structural properties of the primary medial knee ligaments. *Am J Sports Med*. 2010;38(8):1638-1646. doi:10.1177/0363546510363465

Wilson WT, Deakin AH, Payne AP, et al. Comparative analysis of the structural properties of the collateral ligaments of the human knee. *J Orthop Sports Phys Ther*. 2012;42(4):345-351. doi:10.2519/jospt.2012.3919

Winkelstein, B.A. (Ed.). Orthopaedic Biomechanics (1st ed.). In: Thomopoulos S, Genin GM. Tendon and Ligament Biomechanics. CRC Press. 2013, pp.49-74. https://doi.org/10.1201/b13733

Woo SL, Hollis JM, Adams DJ, et al. Tensile properties of the human femur-anterior cruciate ligament-tibia complex. The effects of specimen age and orientation. *Am J Sports Med*. 1991;19(3):217-225. doi:10.1177/036354659101900303

Yoganandan N, Arun MW, Pintar FA, Banerjee A. Lower Leg Injury Reference Values and Risk Curves from Survival Analysis for Male and Female Dummies: Meta-analysis of Postmortem Human Subject Tests. *Traffic Inj Prev*. 2015;16 Suppl 1:S100-S107. doi:10.1080/15389588.2015.1015118